Xstrings: 3D printing cable-driven mechanism for actuation, deformation, and manipulation

JIAJI LI, CSAIL, MIT, United States
SHUYUE FENG, Zhejiang University, China
MAXINE ALEXANDRA PERRONI-SCHARF, CSAIL, MIT, United States
YUJIA LIU, Tsinghua Univeristy, China
EMILY GUAN, Pratt Institute, Brooklyn, United States
GUANYUN WANG, Zhejiang University, China
STEFANIE MUELLER, CSAIL, MIT, United States

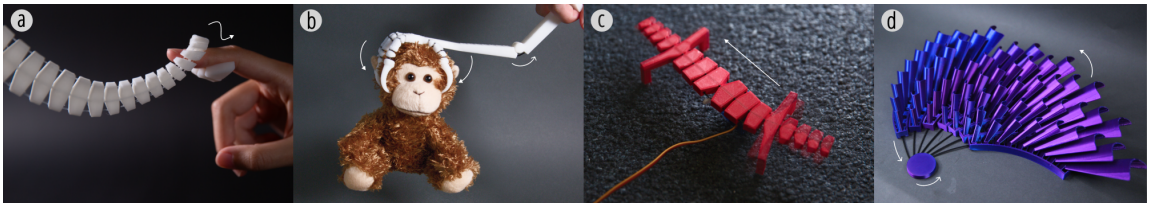

Fig. 1. Xstrings applications include: (a) multi-directional tentacle manipulation, (b) claw with embedded actuation, (c) bio-Inspired lizard robot, (d) dynamic wall sculpture.

In this paper, we present Xstrings, a method for designing and fabricating 3D printed objects with integrated cable-driven mechanisms that can be printed in one go without the need for manual assembly. Xstrings supports four types of cable-driven interactions—bend, twist, coil, and compress—which are activated by applying an input force to the cables. To facilitate the design of Xstrings objects, we developed a design tool that allows users to embed cable-driven mechanisms into the object geometry based on the desired interaction by automatically placing joints and cables at the respective locations. We investigate the effect of different printing parameters on the maximum tensile strain and the extent to which the interaction is repeatable without the cables breaking. The application potential of Xstrings is demonstrated through examples such as manipulable gripping, bionic robot manufacturing, and dynamic prototyping.

CCS Concepts: • **Human-centered computing** → **Human computer interaction (HCI)**; **Systems and tools for interaction design**.

Additional Key Words and Phrases: Cable-driven Mechanism, Personal Fabrication, 3D Printing

Authors' addresses: Jiaji Li, CSAIL, MIT, Cambridge, Massachusetts, United States; Shuyue Feng, Zhejiang University, Hangzhou, Zhejiang, China; Maxine Alexandra Perroni-Scharf, CSAIL, MIT, Cambridge, Massachusetts, United States; Yujia Liu, Tsinghua Univeristy, Beijing, China; Emily Guan, Pratt Institute, Brooklyn, New York, United States; Guanyun Wang, Zhejiang University, Hangzhou, Zhejiang, China; Stefanie Mueller, CSAIL, MIT, Cambridge, Massachusetts, United States.

Manuscript submitted to ACM

ACM Reference Format:
Jiaji Li, Shuyue Feng, Maxine Alexandra Perroni-Scharf, Yujia Liu, Emily Guan, Guanyun Wang, and Stefanie Mueller. 2025. Xstrings: 3D printing cable-driven mechanism for actuation, deformation, and manipulation. In *Proceedings of The ACM Conference on Human Factors in Computing Systems (CHI'25).* ACM, New York, NY, USA, 28 pages. https://doi.org/XXXXXXX.XXXXXXX

1 INTRODUCTION

Prior HCI research has focused on integrating mechanisms into physical objects to enable the creation of dynamic, articulated, and shape-changing structures. To achieve different types of dynamic interactions, researchers have explored various mechanisms to support compliant [27, 52], elastic [12, 42, 47], bi-stable [38, 60], and shape-memory [31, 41] fabrication, allowing users to customize dynamic devices and tangible interfaces.

Cable-driven mechanisms have emerged as a cornerstone in modern robotics, where the delicate interplay of cables to transmit forces and motions offers a unique blend of precision and adaptability. Their inherent lightweight nature and flexibility make them indispensable in diverse applications, ranging from robotic actuation [43] to the development of intricate control systems [45]. For instance, Nikafrooz et al.[34] designed a robotic hand with cables embedded in each finger to mimic the function of tendons, while Colan et al.[4] leveraged similar principles in crafting advanced surgical tools.

Despite their advantages, designing cable-driven mechanisms can be inherently challenging. Achieving a specific desired motion requires precise positioning of the cables and their connection points within the geometry of the main structure, as well as careful adjustment of tension levels. To streamline the design process of such complex mechanisms, researchers have developed various optimization algorithms. For example, Megaro et al.[26] and Li et al.[21] introduced optimization-based methods for the inverse design of cable-driven kinematic chains and trees. These methods have demonstrated the capability to generate a wide range of output motions, including realistic character animations and the development of actuated grippers, thereby expanding the versatility and application potential of cable-driven systems.

While existing design tools provide optimization solutions for cable layouts to achieve the desired motion of an object, the fabrication of such cable-driven mechanisms remains a challenging manual task. This process often involves creating numerous small holes, meticulously threading cables through these holes, and tying knots at precise locations—efforts that are both time-consuming and labor-intensive. Furthermore, the handcrafted nature of these mechanisms poses significant challenges in achieving the precision required for accurate motion trajectories, limiting reproducibility and consistency when producing identical copies of the same structure.

To address these challenges, we present Xstrings, a method that fully automates the integration of cable-driven mechanisms with 3D object geometries, enabling one-step fabrication using dual-material FDM 3D printing. Xstrings supports four types of cable-driven interactions—bend, twist, coil, and compress—which are activated by applying an input force to the cables. To facilitate the design of Xstrings objects, we have developed a design tool that allows users to embed cable-driven mechanisms into 3D objects based on the desired motion by automatically placing cables and joints. This approach enables the automation of cable-driven mechanisms without requiring lengthy production times or manual labor while maintaining the precision of the final object. We investigate how different printing parameters (temperature and printing speed) impact the quality of the printed cable. With the optimized parameters, we further test the maximum tensile strain the mechanisms can sustain before cable breakage and assess the repeatability of the cable-driven interactions. We demonstrate the potential applications of Xstrings through a variety of 3D-printed examples, including advanced dynamic fashion design, bionic robot manufacturing, and interactive prototyping.

In summary, our contributions are:

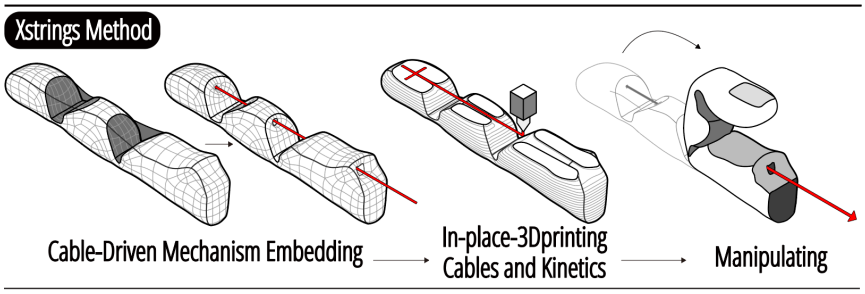

Fig. 2. Embedding cable-driven mechanism with the Xstrings workflow.

- An automated, one-step fabrication approach for 3D printing cable-driven mechanisms, by printing embedded cables, objects, joints, and linkages all at once without the need for manual assembly.
- An interactive design tool that incorporates cable-driven mechanisms into a target structure by decimating it into a user-defined number of links, integrating four different motion primitives (bend, coil, twist, and compress) to approximate the target structure, and exporting fabrication files with printing parameters for the internal embedding of the strings.
- A technical evaluation to determine how 3D printing parameters (printing temperature, extrusion, density, and print path) impact the fatigue and maximum tensile strain of the printed cables.
- A variety of 3D-printed example applications that demonstrate the use of Xstrings cable-driven mechanisms, including medical assistant devices, bionic robot manufacturing, and dynamic prototyping.

2 RELATED WORK

2.1 Manipulation Method of Dynamic Fabrications

In the field of personal fabrication, researchers have utilized digital manufacturing tools to create dynamic materials capable of achieving a wide range of movements that would typically require the creation and assembly of complex mechanical structures. There are two main aspects to this line of prior work: research on the development of dynamic structures, which investigates how to impart mobility to objects, and research on actuation methods, which explores how to control the movement of dynamic objects under external forces.

Common dynamic structures in fabrication include springs [12, 13], joints [22, 58], linkages [17, 18, 56], hinges [35, 52], inflatable structures [46, 61], metamaterials [15, 16], and origami-based designs [32, 53]. For example, PneUI [61] achieves various deformation patterns by arranging inflatable bladders in different configurations. Metamaterials have been 3D printed to create mechanisms that can rotate and extend, achieving effects for motion conduction and linkage [11, 15, 16]. Origami, widely used in engineering, can be employed to create structures that have strength values many times higher than those of their constituting materials through folding techniques [8]. Pop-up Print [36] uses a combination of rigid and flexible materials to allow greater freedom in shaping objects, making it suitable for more diverse applications.

Building upon dynamic structures, various actuation methods can be used for the precise execution of different control tasks. Such methods include pneumatic actuation [28, 33, 50], hydraulic actuation [29], cable-driven actuation [21, 23], and magnetic field manipulation [7, 19]. For instance, FlowIO provides a rapid prototyping platform for pneumatic actuation with an integrated pump terminal [50], while Liquid Pouch Motors use low-boiling-point liquids (around

30°C) to achieve inflation and deflation through temperature changes [33]. ConeAct uses shape memory alloys to drive a flexible unit, enabling multi-degree-of-freedom deformations [23]. ZeroN leverages spatial magnetic fields to suspend a small sphere mid-air and control its motion trajectory freely [19], and MechCircuit employs magnets to simulate various mechanical structures, such as gears and springs [7].

Xstrings expands this landscape by enabling the fabrication of over 30 types of print-in-place dynamic structures with the capability for complex motions. Xstrings utilizes one of the simplest actuation methods—tension applied to cables, which can be generated by the user's hand or programmable devices such as stepper motors, to achieve these motions. Its low-cost, low-entry-barrier, and automatic approach to creating dynamic structures and actuation systems opens up new design possibilities for personalized manufacturing.

2.2 String-like Structures in 3D Printing

String-like structures such as hair, fibers, and cables have been widely utilized by HCI researchers in fabrication to enhance the physical properties of printed objects.

Several studies have focused on incorporating existing string-like materials into 3D-printed creations through post-processing methods [25], significantly enhancing functionality in areas such as shape transformation [24, 57], haptics [6], and sensing [39, 54]. For example, Rivera et al.[44] combine 3D printing and textiles to rapidly create rigid objects with embedded flexibility, as well as soft materials with added functionality. Medley[3] embeds everyday objects into 3D-printable designs to achieve a wider range of material properties. PunchPrint [6] and Hybrid Basketry [64] explore post-print processes where fibers are woven into printed objects, facilitating craftsmanship and customization. Similarly, FlexTruss [51] proposes a cost-effective method that integrates various linear materials into 3D-printed nodes to form flexible prototypes. These studies involve manual weaving as a post-processing step using specific techniques, which can be challenging for ordinary 3D printing enthusiasts to learn. Moreover, the production of a large number of repetitive woven structures can result in significant labor costs.

Beyond embedding traditional fiber-like materials into 3D-printed objects, there is a growing interest in fabricating fiber-like structures directly from 3D printing materials. The 3D printing of these elements can be utilized in various applications, ranging from tactile feedback systems and soft robotics to aesthetic or decorative components in design. WirePrint [30] accelerates low-fidelity wireframe previews in the early stages of the design process. Cilllia [37] achieves micro and fine hair-like structures for motion conduction and aesthetic purposes. To further enhance the flexibility of the printing process and realize more kinds of prototypes with hair-like structures, Extruder-Turtle [40] provides a geometry library that simplifies the generation of G-code files for printing on FDM printers. DefeXtiles [9] proposes employing under-extrusion strings to print woven-like textiles.

While these approaches offer rich physical properties, they do not result in the creation of motion systems or actuation mechanisms. The Xstrings method proposed in this paper introduces a mature cable-driven mechanism using a specially designed 3D printing approach. This method enables the printing of "threaded points" (Section 3.3) that are both interconnected and capable of independent movement, thereby providing a vast design space.

2.3 Cable-Driven Mechanisms

Cable-driven mechanisms serve as foundational technology in modern robotics due to their versatility and lightweight characteristics, making them ideal for a wide range of applications [14, 62]. Their inherent lightweight nature and flexibility make these mechanisms indispensable in applications ranging from robotic actuation [43] to the development of complex control systems [45].

Despite their significant advantages, the design process for cable-driven mechanisms is inherently challenging. Achieving specific motion patterns requires precise geometric design of the mechanical components and the configuration of joints, as well as the strategic placement of cables to provide adequate torque. To address these complexities, researchers have developed various optimization algorithms. For instance, Megaro et al.[26] proposed an inverse design approach for cable-driven mechanisms that minimizes the number of required cables and control forces while achieving desired input motions. Similarly, Li et al.[21] introduced an inverse design strategy to accomplish push and pick-and-place tasks, expanding the possibilities for handling multiple tasks and coordinating multiple cables simultaneously. Shirafuji et al.[49] present a method for designing noncircular pulleys that constrain joint motion by adjusting wire contact points to achieve specific movement ratios in a robotic leg, while Zhang et al.[63] extend this work by proposing a method for designing non-circular pulleys to enable task-defined, nonlinearly coupled tendon-driven actuation, allowing a single motor to control multiple tendons in complex robotic systems.

While existing design tools provide optimization solutions for cable layouts to achieve the desired motion of a target object, the actual fabrication process of such cable-driven mechanisms still presents considerable challenges. Typically, the process requires precise drilling, careful threading of cables through multiple small holes, and secure knotting at specific points. These steps are not only time-consuming and labor-intensive but also demand high manual skill, with any errors potentially compromising the reliability and consistency of the final product. To address these issues, the MoReCa grasper utilizes Lego-like modular and reconfigurable joints to achieve different functionalities without altering the main structure [20]. OpenRST focuses on robot-assisted minimally invasive surgery (RMIS), presenting an open platform for low-cost, biocompatible, and customizable robotic surgical tools [4]. While these methods have improved assembly efficiency and reduced manufacturing costs to some extent, they have not fundamentally addressed the design and labor costs associated with the assembly of cables and mechanical structures.

Despite the numerous advantages of cable-driven systems, the complexity of their design processes and the labor-intensive nature of their assembly remain significant challenges, driving an increasing demand for automation in their production. Xstrings addresses this challenge by integrating 3D printing technology into the production of these systems. By leveraging advanced design tools, Xstrings enhances the design efficiency of cable-driven mechanisms and utilizes integrated manufacturing to achieve zero manual processing and assembly, thereby optimizing the fabrication process and improving precision.

3 XSTRINGS METHOD

The creation of 3D-printed cable-driven mechanisms involves three main challenges: (1) laying out the cable along the mechanism; (2) integrating joints and anchors into the print to enable the desired motion of the main structure when the cable is activated; and (3) defining suitable 3D-printing parameters.

3.1 Laying Out the Cable for the Mechanism

To start, we identify the key components that need to be included in an Xstrings object, referencing classic cable-driven mechanisms. Typically, there are three primary components used to connect a cable to a mechanical structure: (1) **Anchor Points**, (2) **Threaded Points**, and (3) **Exposed Points**, as illustrated in the example of a cable-driven finger in Fig. 3. Below, we introduce the characteristics of each component and provide a detailed explanation of their corresponding manufacturing techniques in Xstrings.

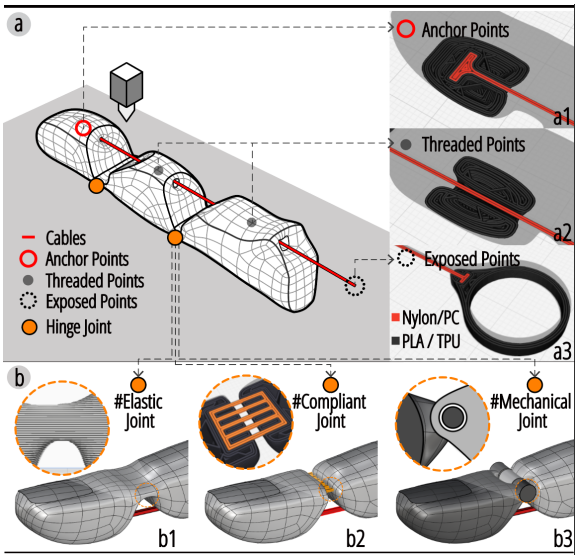

Fig. 3. (a) Three types of relationships between cables and mechanical components: Anchor Points, Threaded Points, and Exposed Points. (b) Three types of hinge joints as options: Elastic, Compliant, and Mechanical.

Anchor Points: The primary objective of a cable-driven mechanism is to achieve precise and real-time control of the end effector (in our example, the fingertip) using cables. In traditional manufacturing methods, this is often accomplished by tying knots to secure the cable. However, since tying knots is not a natural capability of 3D printers, we propose an alternative method for creating anchor points. In our approach, the endpoint of a cable is shaped into a T-shaped anchor and securely fixed in place by the surrounding material, as shown in Fig.3. Our "Anchor Points" allow the surrounding structure to attach firmly to the T-shaped endpoint of the cable without relying on thermal adhesion between different 3D-printed materials, which could easily lead to separation if the materials do not fuse successfully[2].

Threaded Points: In the context of cable-driven mechanisms, “Threaded Points” are locations where a cable passes through holes within the surrounding 3D structure, allowing rectilinear (sliding) motions to occur when the cables are actuated. Enabling such motion is the main technical challenge that our parameter optimization scheme addresses. Threaded points are traditionally created by drilling holes in a structure and manually threading cables through the holes. However, enabling rectilinear motions with cable threading in layer-by-layer 3D printing brings rise to several significant challenges. In particular, friction and resistance between the cable and structure’s 3D printed materials can prohibit smooth rectilinear motions. To address this, in Section 3.3, we identify and introduce suitable printing parameters and materials for the cable-threading process through G-code optimization to improve cable quality and minimize friction and resistance between the printed cables and surrounding material.

Exposed Points: To actuate a cable-driven mechanism, the ends of the cables need to be exposed. These exposed points serve as the interactive input mechanism for a cable-driven structure: by connecting the exposed sections of the cable to various input devices, a force can be efficiently transmitted to the exposed point, which then propagates along the cable to the anchored terminal, driving the entire mechanism. Typical interaction methods for exposed cable endpoints include manual pulling, motor-driven pulling, and gravity. 3D printing unlocks numerous possibilities for

customizing these exposed cable endpoints by incorporating attached "terminal shapes" such as pull rings, spools, or solid weights to suit different interaction methods.

3.2 3D Printing Joints for Cable-Driven Mechanisms

To actuate a cable-driven mechanism, there must also be some form of joint or compliance integrated into the larger 3D object being actuated. In the following subsection, we discuss three types of 3D-printed joints explored in our study.

Elastic Joints: 3D-printed elastic joints leverage the inherent elasticity of common 3D printing materials such as TPU and TPE. One approach to creating 3D-printable elastic joints is to modify certain areas of a 3D object printed with an elastic material to be thinner, making them capable of elastic deformation and effectively functioning as hinges. These joints can be temporarily deformed via a tensing cable and, once the tension is released, return to their original shape, releasing stored elastic energy without permanent deformation.

Compliant Joints: In 3D printing, compliant joints can be created by using an array of multiple thin filaments to form bridges between components of a structure. The stiffness of these filaments can be adjusted to achieve the desired amount of motion in the cable-driven mechanism [52]. Similar to elastic joints, compliant joints have the advantage of simplicity, as they eliminate the need for separate moving parts. These joints are particularly well-suited for lightweight and compact applications.

Mechanical Joints: Unlike elastic and compliant joints, mechanical joints rely on assembling separate, distinct moving components of a structure. In the context of 3D printing, these joints can be fabricated using a print-in-place technique [22], which allows for the creation of mechanical linkages within a single print. These mechanical joints provide robust and reliable connections between components, capable of withstanding significant loads and offering precise control over the movement of large printed components.

By exploring and combining these different types of joints, we can expand the range of applications for 3D-printed cable-actuated mechanical systems and tailor our printed objects to meet the specific needs of various scenarios.

3.3 3D Printing Materials and Parameters for Threading Cable

As mentioned in Section 3.1, by optimizing the print parameters and materials used for FDM 3D printing, we can create high-performance cable-actuated kinetic systems that exploit rectilinear motion between the cables and the body of the printed object. The choice of printing materials and printing parameters greatly affects the quality of the cable, which in turn impacts the motion smoothness of the entire kinetic system. As highlighted in Fig. 4b, we demonstrate that using default printing parameters leads to issues with 3D-printed cable-driven mechanisms, such as drooping and branching. Below, we discuss how we address these challenges through careful selection of print materials and optimization of G-code parameters before printing.

In our cable 3D printing tests, we identified three main issues that can directly lead to the failure:

(1) **Fragile cables**, where the cable itself is too fragile, leading to breakage or fracture during manipulation;
(2) **Fused materials**, where the cable and mechanical components fuse together in undesired locations due to melting during 3D printing, causing separation to become impossible, thus preventing the cable from moving and actuating the mechanism;

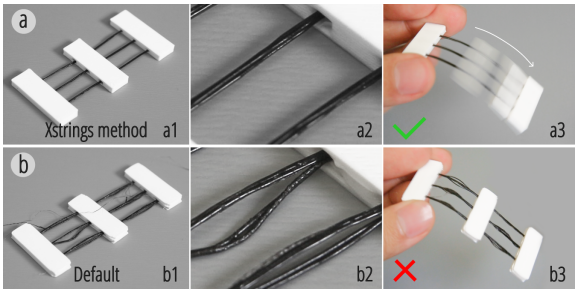

Fig. 4. (a) The 3D printed sample with Xstrings' G-code parameters, result in smooth motions; (b) the sample printed with default settings, which failed in motions.

(3) **Irregular shapes**, where the cable exhibits irregularities such as branching (a single cable into multiple threads, seen in Fig.4b2), uneven thickness, or sagging, which prevent it from passing through holes or result in excessive frictional resistance.

To address these issues, we take several steps as outlined below:

Resilient Cable Materials: Selecting the ideal material for 3D-printed cables requires a balance of high bend resistance and the ability to withstand high tensile stress without undergoing plastic deformation or breakage. Based on filaments datasheets and printing guidelines, we chose Nylon and PC as test materials due to their excellent tensile properties. In practical tests, PC exhibited the highest tensile strength but was prone to plastic deformation and even breakage under repeated bending, making it unsuitable as a cable material. Nylon, on the other hand, demonstrated exceptional bend resistance and maintained stability and durability under repeated bending. Among different types of Nylon (carbon fiber-filled, glass fiber-filled, PA11, PA12 et al.), we selected Nylon 66 for its superior balance of flexibility and strength, making it the most suitable material for Xstrings cables.

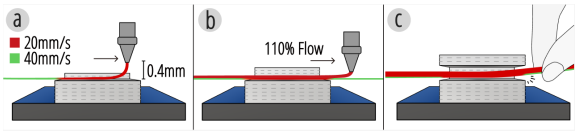

Fig. 5. Xstrings 3D printing strategies and parameters

Materials and Parameters to Avoid Fusion: We print the main structure and joints of the object using a different material than the cable itself. This approach prevents fusion between the cable and its surrounding geometry, which would otherwise occur if the entire object were printed from a single material, as then the matching melting and solidification points would cause the cables and the rest of the structure to bond together. If such fusion were to occur, it would become impossible to separate the components of the print, causing the cable to freeze in places of the print where it needs to be able to slide freely in order to actuate the structure.

We carefully choose materials with sufficiently different melting points to mitigate this problem [2]. We performed tests by 3D printing and cooling cable-driven mechanisms to room temperature, where the cables were printed in Nylon, and the rest of the structures were printed in standard materials such as PLA and TPU. In these tests, illustrated

in Fig. 4, we found the cables can easily become separated from their surrounding geometry either directly from natural shrinkage or with minimal amounts of manual breaking force. As shown in our technical evaluation (Section 8), by carefully adjusting the material spacing to 0.4mm of the first cable layer through G-Code editing, setting the initial layer extrusion to 90%, and controlling the printing temperature (260°C for Nylon) we were able to reduce unintended adhesion to a level that allows the cables to freely move within the mechanism.

Printing Parameters for Cable Straightness: During the FDM 3D printing process, the sections of a cable being printed can be in one of two states: they are either either being suspended mid-air during extrusion, or they are resting on layers of the print have already been extruded. When varying printer settings, we encountered issues such as filament sagging and cable branching, where the cable splits into multiple thin filaments (Fig.4b2). Such cable artifacts can prevent the cable from sliding smoothly along the surfaces of the 3D object and may also block the cable from passing through holes. These issues can be exacerbated if the printing temperature is too high and the printing speed is too slow, as the cable may droop, sag, or even fuse to the print, due to the higher temperature softening the material excessively and gravity pulling down on the softened filament. To mitigate this, we select best performing 3D printing parameters based on a series of experiments (with results shown in Fig. 5).

For the first layer (base) of the 3D print, we reduce the printing speed to 20mm/s (as opposed to the default 70mm/s) and set the bridging speed to 40mm/s, ensuring that the balance between temperature and speed prevents drooping or other artifacts. We also set the extrusion rate to 90% to ensure that any bridges on this base of the 3D print remain perfectly horizontal without sagging. For subsequent layers after the base is printed, we used a speed of 20mm/s for both the printing and the bridging speed, and a 110% extrusion rate. This enables better layer and filaments fusion, avoiding the cable from branching by not fusing with itself.

Evaluation: To further evaluate our choices of print parameters, we compare two versions of the same cable-driven mechanism which consists of a block threaded with 3 cables that should freely slide back and forth between two endpoints. We printed one sample using Xstrings' G-code parameters (as shown in Fig. 4a) and the other using the default printer settings (as shown in Fig. 4b). By testing these samples, we found that our method effectively avoids the issues discussed in this section. Our approach allows the intermediate blocks to move smoothly along the cables, thereby providing reliable manufacturing support for the basic units of the cable-driven mechanism. In the subsequent Evaluations section, we further investigate the force limits of the cables, perform thermal fusion tests on different materials, and explore the impact of printing parameters on cable quality through a variety of experiments.

4 MOTION PRIMITIVES

In order to automate the construction of a variety cable-driven 3D-printable mechanisms, we need to formalize their motion. In mechanical engineering, a "pair with one degree of freedom" (one-DOF pair) is the most fundamental type of mechanism that allows relative motion, comprising three motions: the Revolute pair, Screw pair, and Prismatic pair [1]. In the context of cable-driven mechanisms, a single mechanical object can incorporate multiple one-DOF pairs. We designed four fundamental one-DOF motion primitives: Bend, Coil, Twist, and Compress, as shown in Fig. 6, focusing on four common motions that feature in many existing cable-driven mechanisms. We illustrate these motions on an input geometry of a rectangular cuboid with dimensions of 100mm in length (L = 100mm), 15mm in width (W = 15mm) augmented with cables, joints, gaps and holes that allow for actuation using a cable-driven mechanisms. below, we detail the structure of these motion primitives and their corresponding designs for FDM 3D printing, and show they

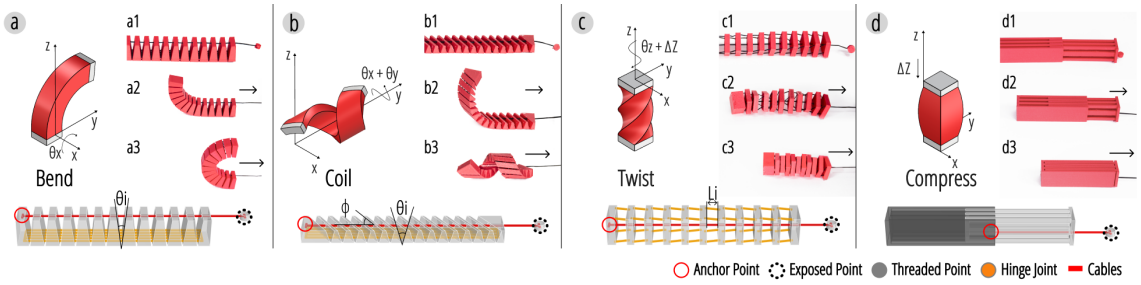

Fig. 6. Four kinds of basic motion primitives of Xstrings

can be combined to achieve a large design space for XStrings objects. Later in the Design Tool section, we show how these primitives can be parameterized and combined to create a variety of different user-defined cable-driven motions.

4.1 Bend

The Bend Primitive, shown in Fig. 6, comprises n joints (in our example, we set $n = 12$) and a single driving cable, with each pair of links allowing rotational motion between them. The rotational angle at each joint is θ_i , which can be controlled by the size and shape of the gap between the two links. We set $\theta_i = \frac{theta}{n}$ so that the total bending angle about the x-axis $theta = \sum_{i=1}^{n} \theta_i$ (so in our example case, $\theta_i = 15°$,$\theta = 180°$). Then, by fixing one end of the primitive to the origin of the x, y, z axes, we can calculate the position of the endpoint of the bend primitive as:

$$(x, y, z) = \left(0, \frac{L}{\theta} \cdot (1 - \cos\theta), \frac{L}{\theta} \cdot \sin\theta\right). \tag{1}$$

This bend-primitive structure is designed using the parametric design tool Grasshopper. We started the design process by generating a single triangular prism with an internal angle of θ_i and then duplicate them n times in a linear array. We then use these triangular prism to cut the input geometry (Boolean Difference) to create n gaps on the geometry, remaining $n + 1$ links. We also design a compliant bridging joint that connects each link in series, enabling rotational motion through the deformation of the flexible material. Finally, using the method described in Fig. 6, holes for the cable within the links are generated to ensure that the cable can transmit force directly to the effector's endpoint, thereby driving the motion of the entire bend primitive.

4.2 Coil

Building on the Bend Primitive, we developed a Coil Motion Primitive, as illustrated in Fig. 6, by adjusting the angles between the primitive's segments. Unlike the Bend primitive, the gaps in the Coil form an angle ϕ with the y-axis direction of the input geometry. This causes the movement of the Coil to no longer directly align with the direction of the x-axis when actuated, but rather results in a non-axis aligned helical coiling motion. As each segment bends by θ_i, the overall shape coils along the y-axis (in this case, the y-axis lines up the structure's own helical axis). The primary parameters for this coil primitive include the number of turns N, radius r, and spring length D.

$$\begin{cases} N = \dfrac{\theta}{2\pi}, \\ r = \dfrac{L \cdot (\cos\phi)}{N \cdot 2\pi}, \\ D = \sqrt{L^2 - (2\pi r N)^2}. \end{cases} \tag{2}$$

Therefore, starting at the origin, the final position of the Coil primitive's endpoint is

$$(x, y, z) = \left(\sqrt{L^2 - (2\pi r N)^2},\ r \cdot \cos(2\pi N),\ r + r \cdot \sin(2\pi N)\right). \tag{3}$$

To 3D model a coil primitive, the modeling workflow is of great similarity to that of the bend primitive. We similarly use n triangle prisms to cut the input geometry. The difference is that, before cutting, triangular prisms are rotated by an angle of ϕ, creating a $(90 - \phi)$-degree angle between the gap direction and the geometry's direction. On this basis, we then add cables and joints, which serve as the driving mechanism and movable structure for the entire primitive.

4.3 Twist

The Twist Primitive is structured as a spring that twists around the z-axis while simultaneously shortening its length during actuation. As illustrated in Fig. 6, when the twist primitive is driven, it coincides the behavior of a spring that contracts in length when rotated around its own longitudinal axis.

The Twist Primitive consists of a continuous helical structure characterized by its length L, radius r, and extreme twist angle θ. The twisting motion is defined by the angular displacement of the endpoint of the structure θ_z around the z-axis, which causes the structure to compress Δz along its axis of rotation. As the structure twists, each incremental rotation of $\Delta\theta_z$ causes a corresponding reduction in length, given by

$$\Delta z = L \cdot \left(1 - \cos\left(\frac{\Delta\theta_z}{2}\right)\right). \tag{4}$$

During the twisting motion, the spring rotates around the z-axis, and its position changes accordingly. The final coordinates of the effect end after a total twist angle of θ_t are

$$(x, y, z) = (0,\ 0,\ L - \Delta z). \tag{5}$$

In the design of the twist mechanism, we use n cuboids of length L_i to cut the input geometry so that each link is also a thin cuboid. When actuated, all the links fully align with each other. Based on this, we position four stiffer compliant joints in a circular array around the cable as the center, with a radius r. When the cable is actuated, these joints convert the force of the links moving closer together into a twisting motion, where

$$\begin{cases} \sin\theta_i = \dfrac{2 \cdot L_i}{r}, \\ \theta_z = \displaystyle\sum_{i=1}^{n} \theta_i \end{cases} \tag{6}$$

4.4 Compress

The compressive structure incorporates a cable into a linear track structure, as shown in Fig. 6d. Due to its simple functions without force transformation, we achieved it with most basic Prismatic pair, which allows only slide motion on z-axis. By pulling the cable, two links compresses along the linear track, reducing its length $\Delta = 0.5L$ to half its original size.

5 DESIGN SPACE

We explore two methods to combine different cable-driven primitives: in series (5.1.1) and in parallel (5.1.2). Both methods offer unique advantages for designing flexible, adaptive structures, enhancing the functional capabilities of 3D-printed mechanisms.

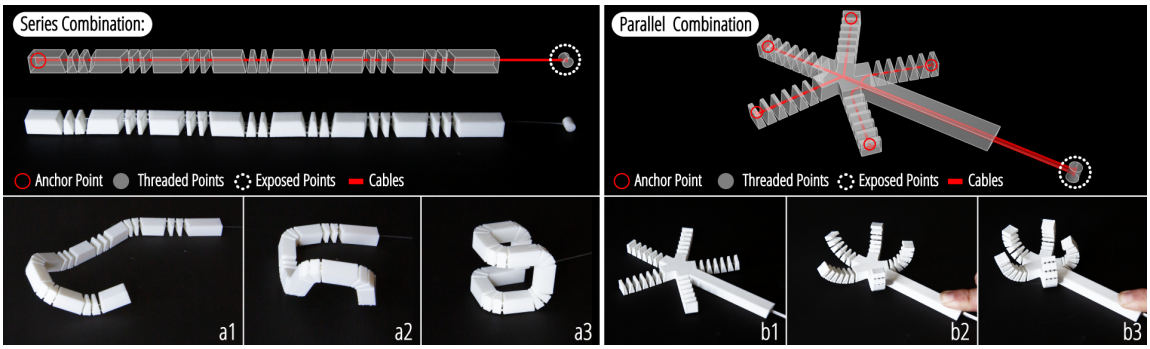

Fig. 7. (a) A series sample designed with 7 Bend primitives, forming a cube frame when actuated; (b) A paralleled sample designed with 7 Bend primitives, forming a cube frame when actuated.

5.1 Dimensional Combination of Primitives

By combining these primitives in series or parallel, we can create complex, adaptive 3D-printed structures tailored to specific functional requirements, demonstrating the versatility and potential of cable-driven mechanisms in soft robotics and advanced manufacturing.

Series Combination

In a series combination, multiple primitives are connected in a sequential manner and driven by a single cable. Cable actuation begins from the farthest end of the mechanism and propagates toward the base, causing cascading deformation along the sequence.

The advantage of the series combination lies in its ability to achieve complex, coordinated movements with minimal control input. Since only one cable is required to drive all connected primitives, the design of sequential mechanisms is more straightforward and compact than parallel mechanisms. This approach is ideal for applications requiring sequential motion of segments of an object, including robotic arms, tentacle-like structures, or bio-inspired soft robots where precise control over motion propagation is necessary (an example of this is given in Section 7.3).

Mathematically, the total driving force and deformation in a series can be mathematically represented as

$$F_{\text{total}} = F_i, \quad \text{while } \Delta L_{\text{total}} = \sum_{i=1}^{n} \Delta L_i, \tag{7}$$

where $\Delta x_i, \Delta y_i, \Delta z_i$ are the deformations of the i-th primitive along the x, y, and z axes, respectively.

An example of a series mechanism is shown in Fig. 7(a). We combine seven bend primitives in series to form a long strip-shaped object, where each bend primitive is capable of bending 90 degrees and can bend in different directions. All these primitives are then controlled by a single cable. As shown in Fig. 7b, c and d, by pulling the cable, this long strip-shaped object will eventually form a square.

Parallel Combination

In a parallel combination, the main cable splits into multiple sub-cables, each connected to a different primitive, but all driven synchronously by a single "central" actuator. This design allows multiple sections of the mechanism to move simultaneously, providing synchronized actuation across all primitives.

The advantage of the parallel combination lies in its ability to achieve simultaneous, coordinated movements, enabling faster and more responsive actuation. This method is ideal for applications that require uniform or synchronized deformations, such as multi-fingered grippers, adaptive surface actuators, or morphing structures.

The synchronization of the sub-cables can be controlled by a central axis, and the relationship between the driving force and the actuation can be mathematically represented as

$$F_{\text{total}} = \sum_{j=1}^{m} F_j, \quad \text{while } \Delta L_{\text{total}} = \Delta L_j, \tag{8}$$

where F_{total} is the total force applied by the main cable, F_j is the force transmitted through each sub-cable, and ΔL_j is the deformation length of the j-th primitive.

We demonstrate a parallel combination in Fig. 7(b). We create a gripper object that consists of a handle with five bending structures forming a star shape at the end. Each of the bending structures is controlled by a different cable, and these five cables are connected in parallel. This means that controlling the final single joining cable can cause all five bending structures to deform simultaneously. As shown in Fig. 7b1, b2 and b3, when this joined parallel cable is pulled by hand, all five bending structures move simultaneously.

5.2 Hole Placement

When determining the placement of threaded points and cables relative to the joints in a structure, it is essential to consider its effect on the force required to actuate the object. If the threaded points are positioned close to the joints, the moment arm (the perpendicular distance from the joint's axis to the line of force) is shortened, meaning that more force is needed to produce the same amount of torque. Conversely, positioning the threaded points farther away from the joints—which may involve higher fabrication complexity—lengthens the moment arm, reducing the necessary force. The structural advantages of keeping threaded points as far from the joints as possible must therefore be balanced against complexity constraints in fabrication.

5.3 Cable Shapes

Compared to traditional cable-driven mechanisms, the customization capabilities of 3D printing allow for the fabrication of cables with various shapes, offering greater design flexibility. In Fig. 8, we present two distinct cable shapes designed to provide haptic feedback and motion control, respectively. The cable in Fig. 8a is designed in a wave-like shape. As it

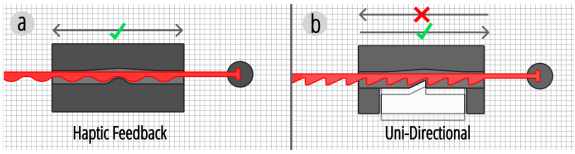

Fig. 8. Two distinct cable shapes designed to provide haptic feedback and motion control

passes through a component's hole, each peak of the wave collides with the underneath bump inside the hole, which

perform a haptic feedback. This design provides a segmented tactile sensation during pulling, which allow users to perceive the distance of the cable actuation.

Inspired by the design principles of zip ties, Fig. 8b features sharper angles at the bends. When pulled and engaged with the underneath ratchet teeth, the cable interlocks with them, preventing reverse movement. The lock can be released by moving the white component downward, allowing for a uni-directional mechanism that can mimic complex motions, such as a snake coiling or a hand grasping. The potential design opportunities enabled by such a uni-directional motion mechanism are explored in greater detail in Section 7.4.

5.4 Embedded-Cable Actuation

In our regular cable-driven mechanism design, objects are actuated by pulling on or manipulating the exposed ends of the cables. However, Xstrings' integrated printing technology enables actuation methods that do not require direct manipulation of the cable endings. We refer to this actuation technique as embedded-cable actuation.

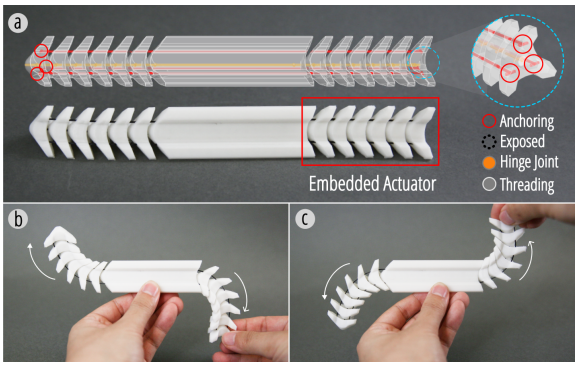

Fig. 9. A sample of a 3D-printed spine with embedded cable actuation, where one of the ends of the spine moves when the opposite end is actuated.

As shown in Fig. 9, the structure contains two segments of spinal-like structures on the left and right, each embedded with three cables and hinge joints, forming an interlinked mechanism. When the middle section is fixed in place, any deformation applied to the tail end results in an opposite deformation at the head end (Fig.9b and c), and vice versa. When the cable ends are exposed, manually controlling the three cables separately to direct the head in a specific direction or perform complex movements, such as swinging or looking around, is quite counterintuitive. The structure design enabled by Xstrings adds possibilities for more natural interaction methods for multi-axis cable-driven mechanisms and provides a more efficient manufacturing approach for cable-driven embedded interlinked mechanisms. We will further introduce this in an application form in 16.

6 DESIGN TOOL

Xstrings software uses Rhinoceros 8 as the design environment and Grasshopper as both a computational tool and an intermediary user interface. In general, the user workflow is: input a geometry for embedding cable-driven mechanism; select desired primitives and define the number of segments and specify the angle after deformation; set a curve as input of cable and tune the cable width and shape of end; export and preview the results and generate the printing file.

6.1 User Workflow

Embedding Primitives: After inputting a geometry drawn in the Rhinoceros environment (recommended to be elongated), users can select a primitive from our library (as shown in Fig. 10). The main interface will display the currently edited segment (shown in red) and the other segments (shown in blue). By adjusting the sliders in the interface, users can edit the bending degree and the number of segments of the actuated shape. We provide some pre-tested initial values as references to help users achieve some of our primitive examples. Once users have implemented a primitive in a specific segment, they can add new segments to achieve other primitives. In Fig. 10, the tip of the tentacle is designed as a coil primitive, while the body is designed with bend primitives to both left and right, respectively.

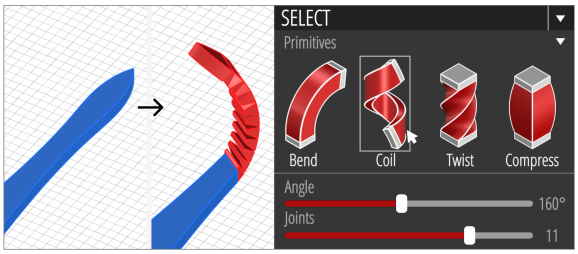

Fig. 10. Primitives Embedding process in Xstrings system.

Modifying the Cable: In this step, users can specify the parameters for each cable, including its shape, width, and thickness, based on the estimated maximum force exerted by the objects. The Xstrings system will then automatically generate a T-shaped anchor point to attach the cable to the furthest end of the end effector. For the threaded points, the design tool offsets the cable's surface by 0.5mm and uses a Boolean difference to create holes for all threaded components. This parametric modeling process maintains a 0.5mm distance between the cable and the wall of the hole, reducing friction while still providing enough control over the cable's path during manipulation. For the exposed points, we offer three types of shapes: dot and ring, which are designed for manual manipulation. The spool can be directly connected to a servos and controlled electrically.

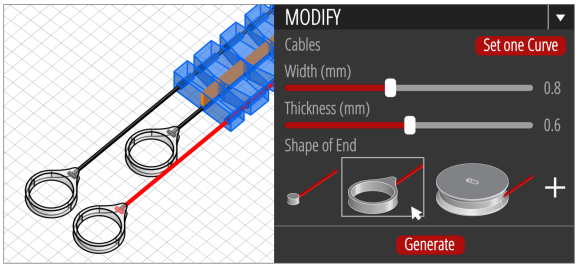

Fig. 11. Cable Modifying in Xstrings system.

Printing Settings for different parts: To increase compatibility and enable the integration of cable-driven mechanisms on any multi-material 3D printer, we opted not to generate G-code for a specific printer model. Instead, we provide parameter settings for different slicing software. We have successfully implemented this functionality on three types

of printers: Ultimaker S5, Ultimaker 3, and Bambu X1. The output files will include three separate files: Main (PLA), Cable1 (Nylon), and Cable2 (Nylon). In our example, "Main" represents the main body of the tentacle, "Cable1" is the first layer of all cables, and "Cable2" represents the remaining layers of the cables. Using the Ultimaker S5 settings as an example, the "Main" part is printed with the settings recommended by the PLA material supplier; "Cable1" is printed at 90% flow rate, 20mm/s regular speed, and 40mm/s bridge wall speed; "Cable2" is printed at 20mm/s speed with a 110% flow rate(Parameters for other FDM 3D printer are provided in the appendix). After slicing and exporting the files, the print can be completed and the manipulation scenarios are shown in Fig. 13.

6.2 Inverse Design

Beyond embedding basic primitives, Xstrings can manipulate elongated blocks into arbitrary curves. In cable-driven robotics, achieving complex curve motions often requires multi-segment control systems, involving multiple motors and cable drive mechanisms connected to various positions [34, 55]. These systems are often large and require complex, labor-intensive assembly processes. To simplify this, Xstrings introduces an automated cable-driven mechanism design tool that enables users to intuitively design such mechanisms using predefined primitives. Our approach abstracts away the complexities of designing individual surface geometry features—such as holes and joints—by generating them automatically. This allows the entire mechanism to be 3D printed in a single step, streamlining the fabrication process.

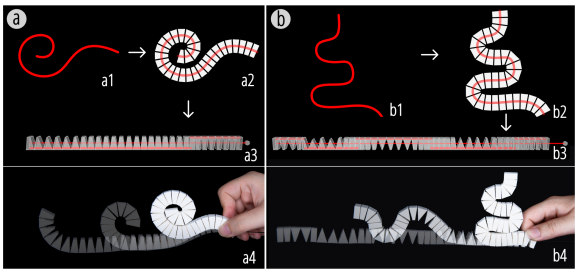

Fig. 12. Inverse design results from 2 different input curves:(a) spiral shape, and (b) serpentine shape.

To abstract away the tedious low-level details of cable-driven mechanism design, we developed an automatic inverse design algorithm that transforms user-input curves into segmented polylines to define the shape of their structure. We do this by replacing each polyline with a series of blocks that are unfolded into straight strip, as illustrated in Fig. 12, and connected with cables and hinge joints.

We use our inverse algorithm to automatically determine the positions of the joints, the gap sizes and the angles. This process ensures that the resulting driven shape and curvature match the user's input precisely. Fig. 12 shows two such printed strips generated from user-defined input curves that are then converted into segmented strips and laid out flat, such that when actuated they deform back into the shape of the original input curve.

7 APPLICATIONS

7.1 Multi-Directional Tentacle Actuation

As mentioned in the previous section, we utilized the design tool to fabricate a controllable tentacle, which consists of 28 components and is printed at the maximum diagonal length of the 3D printing platform. This mechanism incorporates

three cables that control the structure to bend left, coil at the tip, and bend right, respectively (as shown in Fig. 13 b1, b2, and b3).

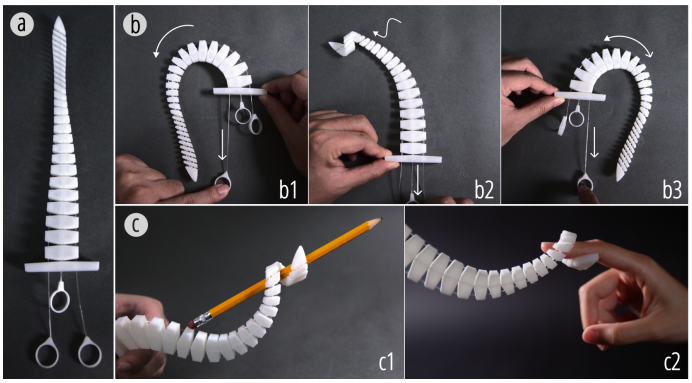

Fig. 13. (a) The assembled tentacle in its neutral position.(b) Controlled movements showing the tentacle's ability to perform bend and coil motions through different cable manipulation.(c) Application scenarios of the tentacle manipulating and grasping objects, showcasing its practical uses in delicate handling tasks.

Due to the real-time responsiveness and accuracy of cable-driven tip control, the tip's coiling action enables better interaction with objects, such as grasping a pencil and wrapping a finger. The design of linked joints allows for precise control of the tip's spatial position, helping it to locate and drag objects more accurately. This case demonstrates how Xstrings utilizes cable-driven mechanisms in 3D-printed dynamic structure to achieve complex motions, providing next-level control and interactivity for FDM 3D printing.

7.2 Bio-Inspired Lizard Robot

In tasks such as exploring unknown areas, environmental modeling, and emergency assistance[5, 10], multiple robots can work collaboratively to quickly accomplish complex operations. However, most current bio-inspired crawling robots, while having significant advantages in traversing complex and diverse terrains[59], are limited in their widespread application and mass production due to high manufacturing costs and complex production processes.

To address this issue, we propose a low-cost bio-inspired lizard robot design based on the Xstrings cable-driven mechanism, as shown in Fig. 14. This robot can be actuated electronically to mimic natural locomotion by alternately bending its body left and right while lifting its back legs. Such movements create a shuffling motion that utilizes surface friction and shifts the center of mass, propelling the robot forward. The precise cable actuation enables the robot to navigate narrow spaces and various terrains effectively. This approach, using a print-in-place manufacturing method and economical components—costing only $1.90 for the motor and $0.40 for the printing material, provides a possible solution for mass production of cable-driven mechanism.

7.3 Fashion and Art Design

3D printing has been widely used by various artists in the design of sculptures, clothing, jewelry, and other fashion pieces. Among them, Herschel Shapiro's repetitive and varied static wall sculptures have garnered a large fan base[48]. We aim to add assembly-free movable structures to these art installations using Xstrings' cable-driven approach. We

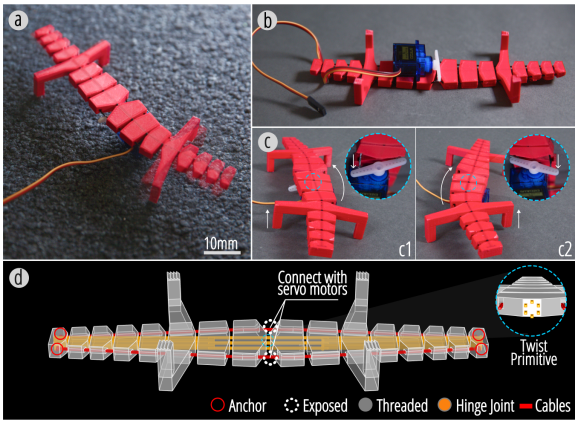

Fig. 14. (a) Xstrings lizard robot demonstrating biomimetic locomotion. (b) Print-in-place design with the robot connected to a Micro Servo Motor (SG90 9G). (c1-c2) Sequential motion showing body bending and twisting.(d) Structural diagram with twist and bend primitives.

designed and fabricated a wing-like dynamic sculpture with Xstrings, as shown in Fig. 15. This structure consists of seven parallel arrays, each comprising eight curved plumes driven by a series of eight bending primitives, all connected by a single cable and actuated via a rotating disk. When the disk is rotated, the plumes transition from a flat position to an upright stance, resembling the spines of a porcupine or the feathers of a bird standing up. We printed this structure with Silk PLA Filament of dual colors, causing the plumes to shift colors from blue to purple as they move. This piece demonstrates the application of Xstrings in the field of art and fashion, creating dynamic, interactive, visually appealing, and easy-to-actuate structures.

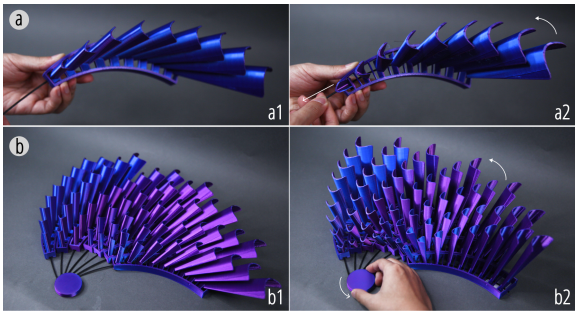

Fig. 15. A Xstrings dynamic sculpture, which could be actuated with a disk.

7.4 Claw with Embedded Actuation

In this section, we designed a cable-driven bird claw with an embedded actuation mechanism to fully explore the Xstrings design and fabrication space. This print-in-place structure consists of four fingers, each composed of five series of bending primitives connected by compliant joints. The four fingers are arranged in a parallel configuration and actuated by a single cable. Additionally, there is a mechanical joint lower down in the arm of the claw, allowing the

elbow of the structure to bend. This is a fully embedded, self-contained mechanism (as described in section 5.3), so instead of the user or a motor directly engaging with the exposed cable, the bending of the elbow itself pulls on the cable, causing the claw to grip. This design allows the user to pick up and transport objects by applying a single force to the elbow of the arm. Due to the ratchet design of the cable shape (Section 8), the bird claw only tightens and does not release during this process, ultimately achieving a firm grip on the object.

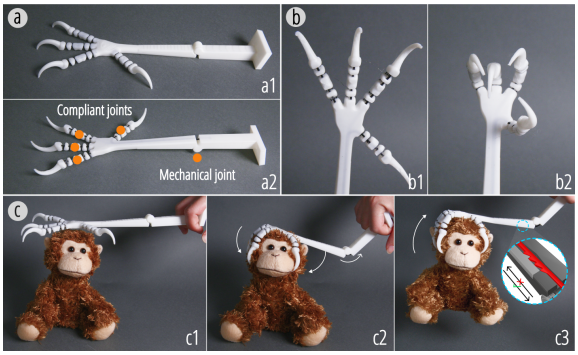

Fig. 16. (a) Design of the claw, featuring four fingers with compliant joints and an elbow with mechanical joint.(b) Display of the claw fingers in open and closed positions.(c) The operation of the claw grasping an object by bending the elbow to drive the cable; due to the ratchet design of the cable, the claw does not release during this process.

8 EVALUATION

8.1 Assessing Cable Properties through 3D Printing Parameter Tuning

To gain a comprehensive understanding of the influence of print temperature and speed on the quality of embedded cables in 3D printing, we conducted a series of controlled experiments to identify the optimal parameters for producing high-quality cable embeddings. While other parameters like nozzle diameter and layer height may also influence print quality, we focus here on temperature and speed as they have the most substantial and easily measurable impact on the resulting cable integrity.

All evaluations were performed using printed specimens that were subjected to different combinations of print temperatures and speeds. Print temperatures were set at 240°C, 260°C, and 280°C, while print speeds varied from 10 mm/s to 30 mm/s. The resulting cable quality, shown in Table 1, was categorized into three levels: “Failed,” “Defective,” and “Optimal,” based on visual inspection and the integrity of the embedded cables.

Print Temperature: Print temperature plays a crucial role in determining the quality of the embedded cables. At a lower temperature of 240°C, the quality of the cables ranged from “Defective” at lower speeds (10 mm/s and 15 mm/s) to “Failed” at higher speeds (20 mm/s to 30 mm/s). The optimal print temperature for achieving high-quality cables was found to be 260°C. At this temperature, the embedded cables demonstrated “Optimal” quality at print speeds of 10 mm/s to 20 mm/s. However, as the speed increased to 25 mm/s, the quality decreased to “Defective,” and at 30 mm/s, it resulted in “Failed” prints. At a higher temperature of 280°C, the quality was generally poor, with “Defective” observed at speeds of 10 mm/s and 15 mm/s, and “Failed” quality at speeds of 20 mm/s and above.

Table 1. Results of cable prints with different printing parameters.

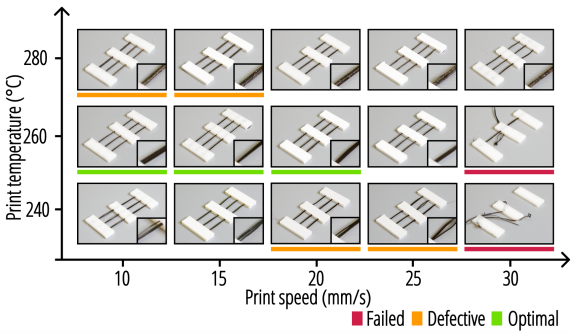

Print Speed: The print speed also significantly affects cable quality. Lower print speeds, specifically 10 mm/s and 15 mm/s, yielded better results across different temperatures, particularly at 260°C where the cable quality was "Optimal." However, as the speed increased to 20 mm/s, the prints remained "Optimal" at 260°C but were "Defective" at other temperatures. Speeds of 25 mm/s and 30 mm/s consistently produced "Defective" or "Failed" prints across all temperature settings, indicating that higher print speeds adversely impact the quality of the embedded cables.

Through our technical analysis, we found that the optimal combination for high-quality cable embedding is a print temperature of 260°C combined with a print speed between 10 mm/s and 20 mm/s. Print speeds exceeding 15 mm/s, especially at temperatures lower than 260°C or higher than 280°C, tend to result in lower quality or failed prints.

8.2 Tension Limits

Table 2. Ultimate tensile force of cables with different width from 0.4mm to 2mm.

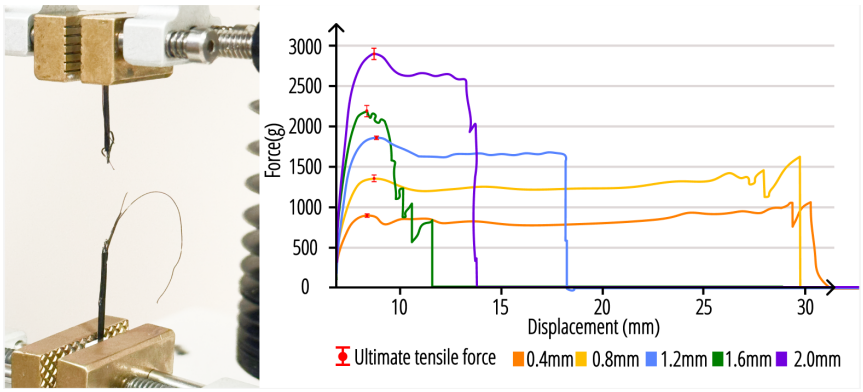

In this experiment, samples were fabricated using a combination of Nylon and Polylactic Acid (PLA) materials through 3D printing. Nylon serves as the cable, anchored at both ends within the PLA. For each width, shown in Table 2,five samples were printed and tested five times, with the resulting curves representing the average of these experiments.

Mathematical Model: In our 3D printing setup, the minimum printing path for the filament is $w_i = 0.4mm$, and so the width of the filament is $w = n \times w_i$, where n is an integer. When n is even, the filament is formed by two passes of 3D printing, resulting in a more uniform mass distribution, and the break usually occurs in the middle of the filament. When n is odd, the filament is more likely to break closer to one of the endpoints due to uneven mass distribution.

To understand the influence of width on the tensile force limit, we assume the cross-section of the filament is rectangular. The cross-sectional area A can be represented as the product of the filament width w and thickness t:

$$A = w \times t. \tag{9}$$

Therefore, the tensile force limit F is proportional to the cross-sectional area, which can be expressed as

$$F \propto A = w \times t. \tag{10}$$

This formula indicates that as the filament width increases, the cross-sectional area also increases, allowing the filament to withstand greater tensile forces.

Effect of Width on Tensile Force Limit: The experimental data shows that, as the filament width increases, the tensile force limit increases significantly. For example, a filament with a width of 2.0mm (purple curve) has a tensile force limit of about 2800g, whereas a filament with a width of 0.4mm (orange curve) has a tensile force limit of only 800g. This demonstrates that a larger cross-sectional area allows the filament to withstand higher tensile forces.

When n is even, the printing path is more uniform, and the filament usually breaks in the middle. When n is odd, the filament is more likely to break near one of its endpoints. This suggests that the tensile properties of the filament are significantly affected by the printing path and the distribution of the material.

Limitation at the Anchor Point: When the filament width $w > 1.6mm$, the Anchor point tends to detach, indicating that the tensile force limit exceeds the PLA material's capacity at the anchor point. At this point, the limiting factor for the cable-driven mechanism shifts from the strength of the Nylon filament to the strength of the PLA anchor. This observation is critical for designing cable-driven mechanisms.

The experimental data and mathematical model indicate that the filament width significantly affects the tensile force limit. As the width increases, the cross-sectional area enlarges, and the tensile force limit increases accordingly. However, when the width reaches a certain threshold (e.g., 1.6mm and above), the limiting factor shifts from the strength of the filament to the strength of the PLA anchor points. These findings provide important guidance for the design and optimization of cable-driven mechanisms in 3D printing.

8.3 Fusion Test between Different Materials

In this experiment, we evaluated the fusion capability between six common 3D printing materials. Generally, better fusion capability indicates that, in multi-material 3D printing, the materials are less likely to separate from each other. Some multi-material 3D printing studies attempt to enhance fusion capability to increase the strength of multi-material components [2]. In contrast, we aim to identify two materials with poor fusion capability to enable the printing of movable threaded points in Xstrings.

For this experiment, we selected six off-the-shelf 3D printing materials: Nylon, PC, TPU, ABS, PETG, and PLA. The printing parameters were set to the default settings in CURA. The experiment involved multi-material printing by pairing each material with every other material, with three samples printed for each pair. The test samples were 2mm-high blocks, with the first 1mm printed using the first material and the second 1mm printed using the second

Table 3. Fusion test result of every two materials.

	PLA	Nylon	PC	TPU	ABS	PETG
PLA						
Nylon						
PC						
TPU						
ABS						
PETG						

Naturally Detach Manually Separate Inseparable

material. After printing and cooling, we attempted to separate the two materials, and the results were recorded in [2]. We categorized the results into three types: the two materials naturally separated after printing and cooling, could be manually separated, or could not be separated. "Cannot be separated" means that when forced apart, the break did not occur at the fusion layer but within one of the materials. As shown in the figure, the experiment results indicate that using PLA and Nylon or PC and Nylon results in natural separation. This means that using these two materials in Xstrings will achieve the best effect.

8.4 Fatigue Limits test of Cables

We used a 28BYJ-48 Step Motor to conduct a fatigue limits test on the Xstring. The servo's stepping parameter is set to 540 (out of 2048 per full revolution). In other words, we actuate a driving rod to pull the cable along an arc of 90 degrees. The speed parameter is set to 15 revolutions per minute, with each loop taking a total of 10 seconds: 4 seconds upward, 1 second pause, 4 seconds downward, and another 1 second pause. The experiment lasted for a total of 7 days and 8 hours, with over 60,000 cycles, eventually breaking at the connection point between the cable and the driving rod.

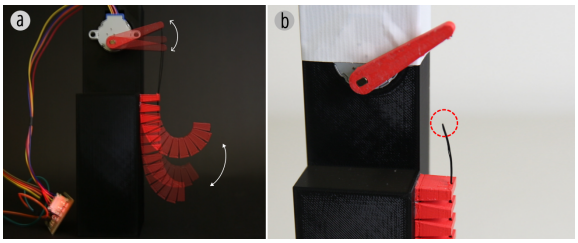

Fig. 17. Fatigue limits test scenario and final breaking points.

9 LIMITATIONS AND FUTURE WORK

We next address the limitations within our work and explore potential directions for future research.

9.1 Limited Success Rate of Elastic Joints

Another limitation lies in the low success rate of printing with elastic materials. Specifically, when using TPU with multi-extruder 3D printers, the printing quality is often poor, resulting in stringing within holes. This stringing obstructs the intended printing path of the nylon cable, preventing the threaded points from moving smoothly and freely. As shown in the figure, two elastic material samples were successfully fabricated, but their success rate is only around 30%.

Additionally, special printing parameters need to be adjusted for different geometries to achieve acceptable quality. Due to these challenges, we have not integrated this type of structure into our software tool. Future work will continue to explore this area, aiming to develop new fabrication strategies for cable-driven soft robotics, where the effective use of elastic materials could provide significant advantages.

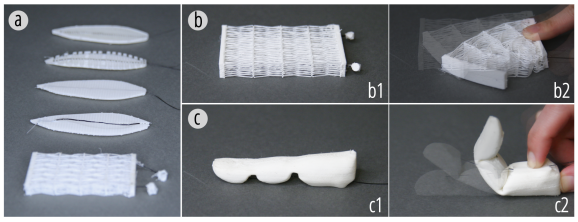

Fig. 18. (a)Majority of failed samples of elastic Xstrings prints.(b,c) Two rare successful prints.

9.2 Only Flat-planar Cables

Despite Xstrings' significant advancements in the automated integration of cable-driven mechanisms into 3D objects, our current approach is limited by the constraints of 3D printing technology. Specifically, the cables in Xstrings can only be printed on the xy-plane. This limitation stems from the extrusion process of FDM 3D printers, where cables need to be printed layer by layer. Stacking material along the z-axis makes the cable very fragile due to the inadequate interlayer bonding strength of nylon, which is insufficient to withstand repeated tensile forces. Thus, printing high-performance cable materials in three-dimensional space becomes challenging.

As a result, our current approach restricts cable paths to the printing plane to ensure the stability and precision of embedded cable-driven mechanisms. Although the cable layout is planar, the actuated objects can still move in multiple dimensions. Future work could explore advanced multi-axis 3D printing techniques or customized G-code manufacturing methods to overcome this limitation, enabling more diverse and spatially complex cable-driven mechanisms.

9.3 Universality Across Other FDM Printers

The extent to which Xstrings results can be directly applied to other users' set-ups is limited to the selection of printing material and printer model. While our evaluation establishes explicit parameter mapping to our 3D printer (Ultimaker and Bambu) and material choice (Nylon 66, yxpolyer), users may need to perform some calibration steps to precisely align the printing parameters to Xstrings's mechanical properties.

10 CONCLUSION

Our Xstrings method provides a novel approach to 3D printing cable-driven mechanisms, significantly simplifying the fabrication process by integrating cable-driven systems directly into the geometry of 3D-printed objects. Unlike traditional methods that require labor-intensive manual assembly, Xstrings automates the design and fabrication, supporting four types of cable-driven interactions—bend, twist, coil, and compress—using dual-material FDM 3D printing. It enables rapid prototyping and the production of complex dynamic structures without the need for additional assembly.

Xstrings demonstrates its versatility through various applications, such as dynamic fashion accessories, bionic robots, and adaptive prototypes. The technical evaluations we present highlight the effectiveness of different printing parameters

in optimizing the mechanical properties of the embedded cables, addressing challenges related to tensile strain, repeatability, and material fusion. The design tool we developed as part of this method facilitates user-friendly integration of cable-driven mechanisms, allowing for customizable designs suited to a wide range of practical applications.

Overall, Xstrings presents a significant advancement in personal fabrication and robotics, offering a low-cost, efficient, and scalable solution for creating dynamic 3D-printed objects with integrated motion capabilities.

REFERENCES

[1] Cemil Bagci. 1971. Degrees of freedom of motion in mechanisms. (1971).

[2] E Brancewicz-Steinmetz, R Valverde Vergara, VH Buzalski, and J Sawicki. 2022. Study of the adhesion between TPU and PLA in multi-material 3D printing. *Journal of Achievements in Materials and Manufacturing Engineering* 115, 2 (2022).

[3] Xiang 'Anthony' Chen, Stelian Coros, and Scott E. Hudson. 2018. Medley: A Library of Embeddables to Explore Rich Material Properties for 3D Printed Objects. In *Proceedings of the 2018 CHI Conference on Human Factors in Computing Systems* (Montreal QC, Canada) *(CHI '18)*. Association for Computing Machinery, New York, NY, USA, 1–12. https://doi.org/10.1145/3173574.3173736

[4] Jacinto Colan, Ana Davila, Yaonan Zhu, Tadayoshi Aoyama, and Yasuhisa Hasegawa. 2023. OpenRST: An Open Platform for Customizable 3D Printed Cable-Driven Robotic Surgical Tools. *IEEE Access* 11 (2023), 6092–6105. https://doi.org/10.1109/ACCESS.2023.3236821

[5] Micael S. Couceiro, David Portugal, and Rui P. Rocha. 2013. A collective robotic architecture in search and rescue scenarios. In *Proceedings of the 28th Annual ACM Symposium on Applied Computing* (Coimbra, Portugal) *(SAC '13)*. Association for Computing Machinery, New York, NY, USA, 64–69. https://doi.org/10.1145/2480362.2480377

[6] Ashley Del Valle, Mert Toka, Alejandro Aponte, and Jennifer Jacobs. 2023. PunchPrint: Creating Composite Fiber-Filament Craft Artifacts by Integrating Punch Needle Embroidery and 3D Printing. In *Proceedings of the 2023 CHI Conference on Human Factors in Computing Systems (CHI '23)*. Association for Computing Machinery, New York, NY, USA, Article 216, 15 pages. https://doi.org/10.1145/3544548.3581298

[7] Shuyue Feng, Cheng Yao, Weijia Lin, Jiayu Yao, Chao Zhang, Zhongyu Jia, Lijuan Liu, Masulani Bokola, Hangyue Chen, Fangtian Ying, et al. 2023. MechCircuit: Augmenting Laser-Cut Objects with Integrated Electronics, Mechanical Structures and Magnets. In *Proceedings of the 2023 CHI Conference on Human Factors in Computing Systems*. 1–15.

[8] Evgueni T Filipov, Tomohiro Tachi, and Glaucio H Paulino. 2015. Origami tubes assembled into stiff, yet reconfigurable structures and metamaterials. *Proceedings of the National Academy of Sciences* 112, 40 (2015), 12321–12326.

[9] Jack Forman, Mustafa Doga Dogan, Hamilton Forsythe, and Hiroshi Ishii. 2020. DefeXtiles: 3D Printing Quasi-Woven Fabric via Under-Extrusion. In *Proceedings of the 33rd Annual ACM Symposium on User Interface Software and Technology (UIST '20)*. Association for Computing Machinery, New York, NY, USA, 1222–1233. https://doi.org/10.1145/3379337.3415876

[10] Antonio Franchi, Luigi Freda, Giuseppe Oriolo, and Marilena Vendittelli. 2009. The Sensor-based Random Graph Method for Cooperative Robot Exploration. *IEEE/ASME Transactions on Mechatronics* 14, 2 (2009), 163–175. https://doi.org/10.1109/TMECH.2009.2013617

[11] Jun Gong, Olivia Seow, Cedric Honnet, Jack Forman, and Stefanie Mueller. 2021. MetaSense: Integrating Sensing Capabilities into Mechanical Metamaterial. In *The 34th Annual ACM Symposium on User Interface Software and Technology* (Virtual Event, USA) *(UIST '21)*. Association for Computing Machinery, New York, NY, USA, 1063–1073. https://doi.org/10.1145/3472749.3474806

[12] Liang He, Huaishu Peng, Michelle Lin, Ravikanth Konjeti, François Guimbretière, and Jon E. Froehlich. 2019. Ondulé: Designing and Controlling 3D Printable Springs. In *Proceedings of the 32nd Annual ACM Symposium on User Interface Software and Technology* (New Orleans, LA, USA) *(UIST '19)*. Association for Computing Machinery, New York, NY, USA, 739–750. https://doi.org/10.1145/3332165.3347951

[13] Liang He, Xia Su, Huaishu Peng, Jeffrey Ian Lipton, and Jon E. Froehlich. 2022. Kinergy: Creating 3D Printable Motion Using Embedded Kinetic Energy. In *Proceedings of the 35th Annual ACM Symposium on User Interface Software and Technology* (Bend, OR, USA) *(UIST '22)*. Association for Computing Machinery, New York, NY, USA, Article 69, 15 pages. https://doi.org/10.1145/3526113.3545636

[14] Huajie Hong, Jabran Ali, and Lei Ren. 2018. A review on topological architecture and design methods of cable-driven mechanism. *Advances in mechanical engineering* 10, 5 (2018), 1687814018774186.

[15] Alexandra Ion, Johannes Frohnhofen, Ludwig Wall, Robert Kovacs, Mirela Alistar, Jack Lindsay, Pedro Lopes, Hsiang-Ting Chen, and Patrick Baudisch. 2016. Metamaterial Mechanisms. In *Proceedings of the 29th Annual Symposium on User Interface Software and Technology* (Tokyo, Japan) *(UIST '16)*. Association for Computing Machinery, New York, NY, USA, 529–539. https://doi.org/10.1145/2984511.2984540

[16] Alexandra Ion, David Lindlbauer, Philipp Herholz, Marc Alexa, and Patrick Baudisch. 2019. Understanding Metamaterial Mechanisms. In *Proceedings of the 2019 CHI Conference on Human Factors in Computing Systems* (Glasgow, Scotland Uk) *(CHI '19)*. Association for Computing Machinery, New York, NY, USA, 1–14. https://doi.org/10.1145/3290605.3300877

[17] Yunwoo Jeong, Han-Jong Kim, and Tek-Jin Nam. 2018. Mechanism Perfboard: An Augmented Reality Environment for Linkage Mechanism Design and Fabrication. In *Proceedings of the 2018 CHI Conference on Human Factors in Computing Systems* (Montreal QC, Canada) *(CHI '18)*. Association for Computing Machinery, New York, NY, USA, 1–11. https://doi.org/10.1145/3173574.3173985

[18] Han-Jong Kim, Yunwoo Jeong, Ju-Whan Kim, and Tek-Jin Nam. 2018. A Prototyping Tool for Kinetic Mechanism Design and Fabrication: Developing and Deploying M.Sketch for Science, Technology, Engineering, the Arts, and Mathematics Education. *Advances in Mechanical Engineering* 10, 12

(Dec. 2018), 168781401880410. https://doi.org/10.1177/1687814018804104

[19] Jinha Lee, Rehmi Post, and Hiroshi Ishii. 2011. ZeroN: mid-air tangible interaction enabled by computer controlled magnetic levitation. In *Proceedings of the 24th annual ACM symposium on User interface software and technology*. 327–336.

[20] Changsheng Li, Xiaoyi Gu, and Hongliang Ren. 2017. A Cable-Driven Flexible Robotic Grasper With Lego-Like Modular and Reconfigurable Joints. *IEEE/ASME Transactions on Mechatronics* 22, 6 (2017), 2757–2767. https://doi.org/10.1109/TMECH.2017.2765081

[21] Jian Li, Sheldon Andrews, Krisztian G Birkas, and Paul G Kry. 2017. Task-based design of cable-driven articulated mechanisms. In *Proceedings of the 1st Annual ACM Symposium on Computational Fabrication*. 1–12.

[22] Jiaji Li, Mingming Li, Junzhe Ji, Deying Pan, Yitao Fan, Kuangqi Zhu, Yue Yang, Zihan Yan, Lingyun Sun, Ye Tao, and Guanyun Wang. 2023. All-in-One Print: Designing and 3D Printing Dynamic Objects Using Kinematic Mechanism Without Assembly. In *Proceedings of the 2023 CHI Conference on Human Factors in Computing Systems* (Hamburg, Germany) *(CHI '23)*. Association for Computing Machinery, New York, NY, USA, Article 689, 15 pages. https://doi.org/10.1145/3544548.3581440

[23] Yuyu Lin, Jesse T Gonzalez, Zhitong Cui, Yash Rajeev Banka, and Alexandra Ion. 2024. ConeAct: A Multistable Actuator for Dynamic Materials. In *Proceedings of the CHI Conference on Human Factors in Computing Systems*. 1–16.

[24] Min Liu, Yunbo Zhang, Jing Bai, Yuanzhi Cao, Jeffrey M. Alperovich, and Karthik Ramani. 2017. WireFab: Mix-Dimensional Modeling and Fabrication for 3D Mesh Models. In *Proceedings of the 2017 CHI Conference on Human Factors in Computing Systems* (Denver, Colorado, USA) *(CHI '17)*. Association for Computing Machinery, New York, NY, USA, 965–976. https://doi.org/10.1145/3025453.3025619

[25] Eric MacDonald and Ryan Wicker. 2016. Multiprocess 3D printing for increasing component functionality. *Science* 353, 6307 (2016), aaf2093. https://doi.org/10.1126/science.aaf2093 arXiv:https://www.science.org/doi/pdf/10.1126/science.aaf2093

[26] Vittorio Megaro, Espen Knoop, Andrew Spielberg, David IW Levin, Wojciech Matusik, Markus Gross, Bernhard Thomaszewski, and Moritz Bächer. 2017. Designing cable-driven actuation networks for kinematic chains and trees. In *Proceedings of the ACM SIGGRAPH/Eurographics symposium on computer animation*. 1–10.

[27] Vittorio Megaro, Jonas Zehnder, Moritz Bächer, Stelian Coros, Markus H Gross, and Bernhard Thomaszewski. 2017. A computational design tool for compliant mechanisms. *ACM Trans. Graph.* 36, 4 (2017), 82–1.

[28] Takafumi Morita, Ziyuan Jiang, Kanon Aoyama, Ayato Minaminosono, Yu Kuwajima, Naoki Hosoya, Shingo Maeda, and Yasuaki Kakehi. 2023. InflatableMod: Untethered and reconfigurable inflatable modules for tabletop-sized pneumatic physical interfaces. In *Proceedings of the 2023 CHI Conference on Human Factors in Computing Systems*. 1–15.

[29] Takafumi Morita, Yu Kuwajima, Ayato Minaminosono, Shingo Maeda, and Yasuaki Kakehi. 2022. HydroMod: Constructive Modules for Prototyping Hydraulic Physical Interfaces. In *Proceedings of the 2022 CHI Conference on Human Factors in Computing Systems*. 1–14.

[30] Stefanie Mueller, Sangha Im, Serafima Gurevich, Alexander Teibrich, Lisa Pfisterer, François Guimbretière, and Patrick Baudisch. 2014. WirePrint: 3D printed previews for fast prototyping. In *Proceedings of the 27th Annual ACM Symposium on User Interface Software and Technology* (Honolulu, Hawaii, USA) *(UIST '14)*. Association for Computing Machinery, New York, NY, USA, 273–280. https://doi.org/10.1145/2642918.2647359

[31] Sachith Muthukumarana, Moritz Alexander Messerschmidt, Denys J.C. Matthies, Jürgen Steimle, Philipp M. Scholl, and Suranga Nanayakkara. 2021. ClothTiles: A Prototyping Platform to Fabricate Customized Actuators on Clothing using 3D Printing and Shape-Memory Alloys. In *Proceedings of the 2021 CHI Conference on Human Factors in Computing Systems (CHI '21)*. Association for Computing Machinery, New York, NY, USA, 1–12. https://doi.org/10.1145/3411764.3445613

[32] Koya Narumi, Kazuki Koyama, Kai Suto, Yuta Noma, Hiroki Sato, Tomohiro Tachi, Masaaki Sugimoto, Takeo Igarashi, and Yoshihiro Kawahara. 2023. Inkjet 4D Print: Self-folding Tessellated Origami Objects by Inkjet UV Printing. *ACM Trans. Graph.* 42, 4, Article 117 (jul 2023), 13 pages. https://doi.org/10.1145/3592409

[33] Koya Narumi, Hiroki Sato, Kenichi Nakahara, Young ah Seong, Kunihiko Morinaga, Yasuaki Kakehi, Ryuma Niiyama, and Yoshihiro Kawahara. 2020. Liquid pouch motors: printable planar actuators driven by liquid-to-gas phase change for shape-changing interfaces. *IEEE Robotics and Automation Letters* 5, 3 (2020), 3915–3922.

[34] Negin Nikafrooz and Alexander Leonessa. 2021. A Single-Actuated, Cable-Driven, and Self-Contained Robotic Hand Designed for Adaptive Grasps. *Robotics* 10, 4 (2021). https://doi.org/10.3390/robotics10040109

[35] Yuta Noma, Koya Narumi, Fuminori Okuya, and Yoshihiro Kawahara. 2020. Pop-up Print: Rapidly 3D Printing Mechanically Reversible Objects in the Folded State. In *Proceedings of the 33rd Annual ACM Symposium on User Interface Software and Technology* (Virtual Event, USA) *(UIST '20)*. Association for Computing Machinery, New York, NY, USA, 58–70. https://doi.org/10.1145/3379337.3415853

[36] Yuta Noma, Koya Narumi, Fuminori Okuya, and Yoshihiro Kawahara. 2020. Pop-up Print: Rapidly 3D Printing Mechanically Reversible Objects in the Folded State. In *Proceedings of the 33rd Annual ACM Symposium on User Interface Software and Technology*. ACM, Virtual Event USA, 58–70. https://doi.org/10.1145/3379337.3415853

[37] Jifei Ou, Gershon Dublon, Chin-Yi Cheng, Felix Heibeck, Karl Willis, and Hiroshi Ishii. 2016. Cilllia: 3D Printed Micro-Pillar Structures for Surface Texture, Actuation and Sensing. In *Proceedings of the 2016 CHI Conference on Human Factors in Computing Systems*. ACM, San Jose California USA, 5753–5764. https://doi.org/10.1145/2858036.2858257

[38] Athina Panotopoulou, Valkyrie Savage, and Daniel Lee Ashbrook. 2024. Threa-D Printing Tunable Bistable Mechanisms. In *Adjunct Proceedings of the 9th ACM Symposium on Computational Fabrication* (Aarhus, Denmark) *(SCF Adjunct '24)*. Association for Computing Machinery, New York, NY, USA, Article 16, 3 pages. https://doi.org/10.1145/3665662.3673272

[39] Huaishu Peng, François Guimbretière, James McCann, and Scott Hudson. 2016. A 3D Printer for Interactive Electromagnetic Devices. In *Proceedings of the 29th Annual Symposium on User Interface Software and Technology* (Tokyo, Japan) *(UIST '16)*. Association for Computing Machinery, New York, NY, USA, 553–562. https://doi.org/10.1145/2984511.2984523

[40] Franklin Pezutti-Dyer and Leah Buechley. 2022. Extruder-Turtle: A Library for 3D Printing Delicate, Textured, and Flexible Objects. In *Sixteenth International Conference on Tangible, Embedded, and Embodied Interaction*. ACM, Daejeon Republic of Korea, 1–9. https://doi.org/10.1145/3490149.3501312

[41] Katy Pieri, Bailey M. Felix, Teng Zhang, Pranav Soman, and James H. Henderson. 2023. Printing Parameters of Fused Filament Fabrication Affect Key Properties of Four-Dimensional Printed Shape-Memory Polymers. *3D Printing and Additive Manufacturing* 10, 2 (2023), 279–288. https://doi.org/10.1089/3dp.2021.0072 arXiv:https://doi.org/10.1089/3dp.2021.0072

[42] Stefan Pillwein, Johanna Kübert, Florian Rist, and Przemyslaw Musialski. 2020. Design and Fabrication of Elastic Geodesic Grid Structures. In *Proceedings of the 5th Annual ACM Symposium on Computational Fabrication* (Virtual Event, USA) *(SCF '20)*. Association for Computing Machinery, New York, NY, USA, Article 2, 11 pages. https://doi.org/10.1145/3424630.3425412

[43] Sen Qian, Bin Zi, Wei-Wei Shang, and Qing-Song Xu. 2018. A Review on Cable-driven Parallel Robots. *Chinese Journal of Mechanical Engineering* 31, 1 (Aug. 2018), 66. https://doi.org/10.1186/s10033-018-0267-9

[44] Michael L. Rivera, Melissa Moukperian, Daniel Ashbrook, Jennifer Mankoff, and Scott E. Hudson. 2017. Stretching the Bounds of 3D Printing with Embedded Textiles. In *Proceedings of the 2017 CHI Conference on Human Factors in Computing Systems* (Denver, Colorado, USA) *(CHI '17)*. Association for Computing Machinery, New York, NY, USA, 497–508. https://doi.org/10.1145/3025453.3025460

[45] João Cavalcanti Santos, Marc Gouttefarde, and Ahmed Chemori. 2022. A Nonlinear Model Predictive Control for the Position Tracking of Cable-Driven Parallel Robots. *IEEE Transactions on Robotics* 38, 4 (2022), 2597–2616. https://doi.org/10.1109/TRO.2022.3152705

[46] Harpreet Sareen, Udayan Umapathi, Patrick Shin, Yasuaki Kakehi, Jifei Ou, Hiroshi Ishii, and Pattie Maes. 2017. Printflatables: Printing Human-Scale, Functional and Dynamic Inflatable Objects. In *Proceedings of the 2017 CHI Conference on Human Factors in Computing Systems* (Denver, Colorado, USA) *(CHI '17)*. Association for Computing Machinery, New York, NY, USA, 3669–3680. https://doi.org/10.1145/3025453.3025898

[47] Christian Schumacher, Bernd Bickel, Jan Rys, Steve Marschner, Chiara Daraio, and Markus Gross. 2015. Microstructures to Control Elasticity in 3D Printing. *ACM Trans. Graph.* 34, 4, Article 136 (jul 2015), 13 pages. https://doi.org/10.1145/2766926

[48] Herschel Shapiro. 2022. Herschel Shapiro's Artworks. https://www.youtube.com/@HerschelShapiro. Accessed: 2024-09-15.

[49] Shouhei Shirafuji, Shuhei Ikemoto, and Koh Hosoda. 2016. Designing noncircular pulleys to realize target motion between two joints. *IEEE/ASME Transactions on Mechatronics* 22, 1 (2016), 487–497.

[50] Ali Shtarbanov. 2021. Flowio development platform–the pneumatic "raspberry pi" for soft robotics. In *Extended abstracts of the 2021 CHI conference on human factors in computing systems*. 1–6.

[51] Lingyun Sun, Jiaji Li, Yu Chen, Yue Yang, Zhi Yu, Danli Luo, Jianzhe Gu, Lining Yao, Ye Tao, and Guanyun Wang. 2021. FlexTruss: A Computational Threading Method for Multi-Material, Multi-Form and Multi-Use Prototyping. In *Proceedings of the 2021 CHI Conference on Human Factors in Computing Systems* (Yokohama, Japan) *(CHI '21)*. Association for Computing Machinery, New York, NY, USA, Article 432, 12 pages. https://doi.org/10.1145/3411764.3445311

[52] Lingyun Sun, Jiaji Li, Junzhe Ji, Deying Pan, Mingming Li, Kuangqi Zhu, Yitao Fan, Yue Yang, Ye Tao, and Guanyun Wang. 2022. X-Bridges: Designing Tunable Bridges to Enrich 3D Printed Objects' Deformation and Stiffness. In *Proceedings of the 35th Annual ACM Symposium on User Interface Software and Technology* (Bend, OR, USA) *(UIST '22)*. Association for Computing Machinery, New York, NY, USA, Article 20, 12 pages. https://doi.org/10.1145/3526113.3545710

[53] Lingyun Sun, Jiaji Li, Mingming Li, Yitao Fan, Yu Chen, Deying Pan, Yue Yang, Junzhe Ji, Ye Tao, and Guanyun Wang. 2021. 3DP-Ori: Bridging-Printing Based Origami Fabrication Method with Modifiable Haptic properties. In *Adjunct Proceedings of the 34th Annual ACM Symposium on User Interface Software and Technology* (Virtual Event, USA) *(UIST '21 Adjunct)*. Association for Computing Machinery, New York, NY, USA, 74–77. https://doi.org/10.1145/3474349.3480233

[54] Saiganesh Swaminathan, Kadri Bugra Ozutemiz, Carmel Majidi, and Scott E. Hudson. 2019. FiberWire: Embedding Electronic Function into 3D Printed Mechanically Strong, Lightweight Carbon Fiber Composite Objects. In *Proceedings of the 2019 CHI Conference on Human Factors in Computing Systems* (Glasgow, Scotland Uk) *(CHI '19)*. Association for Computing Machinery, New York, NY, USA, 1–11. https://doi.org/10.1145/3290605.3300797

[55] Kazutoshi Tanaka and Masashi Hamaya. 2023. Twist Snake: Plastic table-top cable-driven robotic arm with all motors located at the base link. In *2023 IEEE International Conference on Robotics and Automation (ICRA)*. 7345–7351. https://doi.org/10.1109/ICRA48891.2023.10160995

[56] Bernhard Thomaszewski, Stelian Coros, Damien Gauge, Vittorio Megaro, Eitan Grinspun, and Markus Gross. 2014. Computational Design of Linkage-Based Characters. *ACM Trans. Graph.* 33, 4, Article 64 (jul 2014), 9 pages. https://doi.org/10.1145/2601097.2601143

[57] Guanyun Wang, Tingyu Cheng, Youngwook Do, Humphrey Yang, Ye Tao, Jianzhe Gu, Byoungkwon An, and Lining Yao. 2018. Printed Paper Actuator: A Low-cost Reversible Actuation and Sensing Method for Shape Changing Interfaces. In *Proceedings of the 2018 CHI Conference on Human Factors in Computing Systems*. ACM, Montreal QC Canada, 1–12. https://doi.org/10.1145/3173574.3174143

[58] Guanyun Wang, Ye Tao, Ozguc Bertug Capunaman, Humphrey Yang, and Lining Yao. 2019. A-Line: 4D Printing Morphing Linear Composite Structures. In *Proceedings of the 2019 CHI Conference on Human Factors in Computing Systems* (Glasgow, Scotland Uk) *(CHI '19)*. Association for Computing Machinery, New York, NY, USA, 1–12. https://doi.org/10.1145/3290605.3300656

[59] Ruiqin Wang, Hao Wu, and Jian S. Dai. 2024. A Novel Bio-Inspired Quadruped Crawling Robot with Movable Waist. In *2024 6th International Conference on Reconfigurable Mechanisms and Robots (ReMAR)*. 218–223. https://doi.org/10.1109/ReMAR61031.2024.10617730

[60] Yue Yang, Lei Ren, Chuang Chen, Bin Hu, Zhuoyi Zhang, Xinyan Li, Yanchen Shen, Kuangqi Zhu, Junzhe Ji, Yuyang Zhang, Yongbo Ni, Jiayi Wu, Qi Wang, Jiang Wu, Lingyun Sun, Ye Tao, and Guanyun Wang. 2024. SnapInflatables: Designing Inflatables with Snap-through Instability for Responsive Interaction. In *Proceedings of the CHI Conference on Human Factors in Computing Systems* (Honolulu, HI, USA) *(CHI '24)*. Association for Computing Machinery, New York, NY, USA, Article 342, 15 pages. https://doi.org/10.1145/3613904.3642933

[61] Lining Yao, Ryuma Niiyama, Jifei Ou, Sean Follmer, Clark Della Silva, and Hiroshi Ishii. 2013. PneUI: pneumatically actuated soft composite materials for shape changing interfaces. In *Proceedings of the 26th annual ACM symposium on User interface software and Technology*. 13–22.

[62] Mahmoud Zarebidoki, Jaspreet Singh Dhupia, and Weiliang Xu. 2022. A review of cable-driven parallel robots: Typical configurations, analysis techniques, and control methods. *IEEE Robotics & Automation Magazine* 29, 3 (2022), 89–106.

[63] Wensi Zhang, Barnabas Gavin Cangan, Thomas Buchner, Alexander M Kübler, Ramon Asmus, and Robert K Katzschmann. 2024. Task-defined Pulley Design for Nonlinearly Coupled Tendon-driven Actuation. In *2024 IEEE 7th International Conference on Soft Robotics (RoboSoft)*. IEEE, 220–227.

[64] Amit Zoran. 2013. Hybrid basketry: interweaving digital practice within contemporary craft. In *ACM SIGGRAPH 2013 Art Gallery* (Anaheim, California) *(SIGGRAPH '13)*. Association for Computing Machinery, New York, NY, USA, 324–331. https://doi.org/10.1145/2503649.2503651

A PRINTING SETTINGS FOR DIFFERENT MODEL OF 3D PRINTER

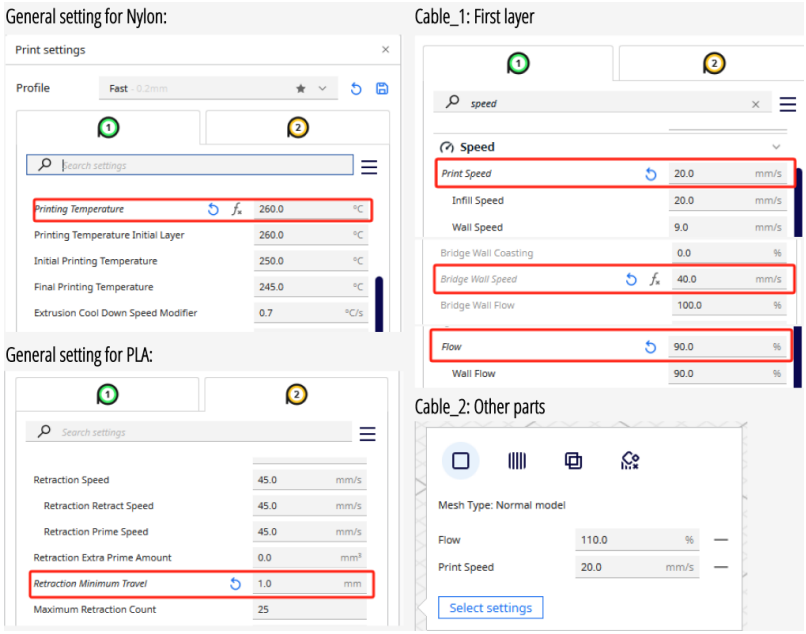

Fig. 19. Settings for Ultimaker 3 and S5

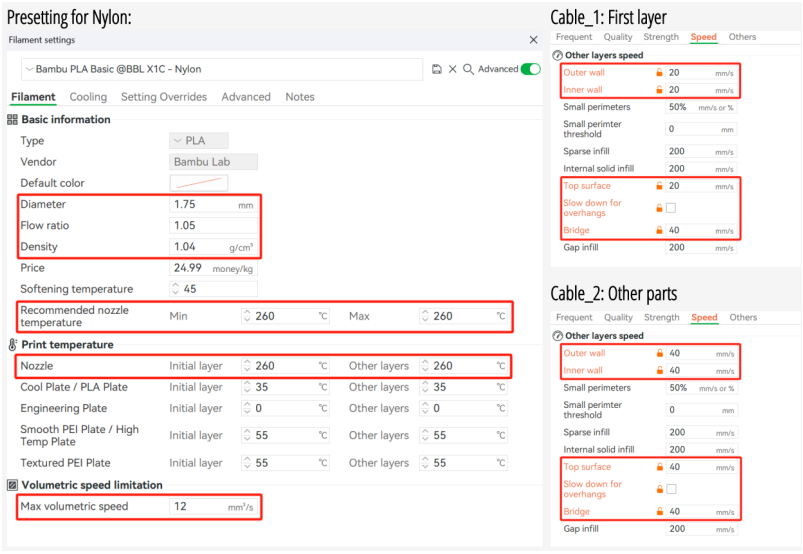

Fig. 20. Settings for Bambu X1